Available online at www.sciencedirect.com

ScienceDirect

Physics Procedia 53 (2014) 90 – 95

Physics Procedia

Thermodynamics of Protein Aggregation

Kenneth L. Osborne[1], Bogdan Barz[1], Michael Bachmann[2], and Birgit Strodel[1,3]*

[1] Institute of Complex Systems: Structural Biochemistry, Forschungszentrum Jülich GmbH, 52425 Jülich, Germany
[2] Center for Simulational Physics, The University of Georgia, Athens, Georgia 30602, USA
[3] Institute of Theoretical and Computational Chemistry, Heinrich Heine University Düsseldorf, 40225 Düsseldorf, Germany

Abstract

Amyloid protein aggregation characterizes many neurodegenerative disorders, including Alzheimer's, Parkinson's, and Creutzfeldt-Jakob disease. Evidence suggests that amyloid aggregates may share similar aggregation pathways, implying simulation of full-length amyloid proteins is not necessary for understanding amyloid formation. In this study we simulate GNNQQNY, the N-terminal prion-determining domain of the yeast protein Sup35 to investigate the thermodynamics of structural transitions during aggregation. We use a coarse-grained model with replica-exchange molecular dynamics to investigate the association of 3-, 6-, and 12-chain GNNQQNY systems and we determine the aggregation pathway by studying aggregation states of GNNQQNY. We find that the aggregation of the hydrophilic GNNQQNY sequence is mainly driven by H-bond formation, leading to the formation of β-sheets from the very beginning of the assembly process. Condensation (aggregation) and ordering take place simultaneously, which is underpinned by the occurrence of a single heat capacity peak only.

Peer-review under responsibility of The Organizing Committee of CSP 2013 conference

Keywords: amyloid aggregation; coarse-grained simulations; replica exchange molecular dynamics; statistical analysis; orientational order parameters; aggregation states

1. Introduction

Diseases such as Alzheimer's disease, Parkinson's disease, type II diabetes, and others share a general characteristic: each of them is associated with the misfolding and subsequent aggregation of soluble peptides and proteins into soluble oligomeric assemblies, and later, into insoluble amyloid fibrils [1–3]. During the past decade compelling evidence has emerged that soluble, low molecular weight oligomers are more toxic than fully formed fibrils [4–7]. The study of protein fragments that retain the essential amyloid characteristics of the full length sequences is attractive because the short peptide length allows for a systematic computational investigation of aggregation kinetics and thermodynamics. One such example fragment is GNNQQNY, a polar heptapeptide from the N-terminal region of the yeast prion protein Sup35 that exhibits amyloidogenic properties similar to the prion-determining domain of Sup35 [8].

The knowledge of the atomic structure of GNNQQNY fibrils [8–10], together with its small size, has led GNNQQNY to become a model amyloid test system for experimental and theoretical studies. One of the first computational studies of GNNQQNY examined the behavior of the trimer using molecular dynamics (MD) simulations at a constant temperature of 330 K and revealed that the in-register parallel β-sheet observed in experiments is stabilized by side-chain hydrogen bonding and π-stacking of the aromatic tyrosine residues [12]. This study was followed by various other simulation studies, which characterized the structures and free energies of small GNNQQNY aggregates ranging from dimers to 20-mers starting from disordered states, or studied the stability of pre-formed GNNQQNY assemblies with cross-β or annular morphologies [13–22].

Given the large time and length scales involved in aggregation, coarse-grained (CG) models provide the possibility of extracting general characteristics of the thermodynamics and kinetics of aggregation. CG models utilized for studying amyloid aggregation include the model by Caflisch and coworkers, where each peptide consists of four spherical backbone beads and six spherical side-chain beads of hydrophobic and hydrophilic nature [24–26], the mid-resolution Shea model with two backbone and one side chain bead per residue [27, 28], discontinuous CG models used in connection with discrete molecular dynamics

*Email address: b.strodel@fz-juelich.de (Birgit Strodel)

Peer-review under responsibility of The Organizing Committee of CSP 2013 conference
doi:10.1016/j.phpro.2014.06.032

[29–33], and the OPEP model by Derreumaux and coworkers that uses a detailed representation of all backbone atoms and reduces each side-chain to a single bead [34–37].

In this paper, we perform REMD simulations using the CG peptide model developed by Bereau and Deserno [38] to investigate the thermodynamics of structural transitions during the aggregation of the 3-, 6-, and 12-chain GNNQQNY systems.[22] Their intermediate resolution level CG force field was shown to be able to fold proteins exhibiting both helical and β conformations with tertiary structures and amino acid sequences different from the one used for parameter tuning [38–40]. The aim of the current study is analyze the structures and thermodynamics during aggregation of the GNNQQNY peptide. The resulting aggregation dynamics in temperature space is characterized in terms of orientational order, secondary structure and aggregation states.

2. Model and Methods

The primary motivation for using a CG model was to reach the greater than microsecond time scales associated with peptide aggregation. The C_β-type CG force field we use here was built to sample a balanced proportion of α-helical and β-extended configurations, with the aim of avoiding a bias toward any particular secondary structure [38]. The backbone is represented by three beads per residue and one bead per side chain with the latter located in the position of the C_β atom. The force field was parametrized to reproduce local, secondary, and tertiary conformations. The nearly atomistic resolution of the backbone beads allows the force field to model physically relevant secondary structures, such as β-sheets and α-helices, without imposing a given secondary structure prior to simulation [38].

To sample the conformational space, we employed the REMD method [23] as implemented in the ESPRESSO simulation package [41]. Each REMD simulation was started from 3, 6, or 12 chains of GNNQQNY peptides placed at random starting positions and in random conformations in a simulation box at a concentration of 80 mM. Each REMD simulation was performed for 500 million time steps per replica, where the initial 100 million steps were used for system equilibration. This results in about 500 ns simulation time per replica. Studies of the 3-chain system used 10 temperature replicas, while the studies of the 6- and 12-chain systems used 16 replicas. Within each temperature thread of our REMD simulations resides a canonical (NVT) simulation. The weighted histogram analysis method (WHAM) combines the data from all replicas to extract the multicanonical ensemble averages [42]. It was used to calculate thermodynamic quantities, such as the heat capacity (C_v), and the average behavior of impact parameters ($\langle P \rangle$) defined as a function of T.

For the characterization of the aggregation behavior, we computed the liquid crystal order parameters P_1 and P_2 to determine the (anti)parallel structural order of the system [13]. This is useful because amyloidogenic sequences are expected to form β-sheets, and thus be aligned in characteristic forms. For the classification of the GNNQQNY oligomers in terms of their

State Name	Oligomeric Species	Population
0	Monomer	3
1	Monomer	1
	Dimer	1
2	Trimer	1

Table I: Definition of the unique aggregation states of a system containing three GNNQQNY peptides.

aggregation state, we analyzed the aggregate size for each structure sampled in our REMD simulations. Here, a single chain is said to belong to a given oligomer cluster if it shares one or more hydrogen bonds with another chain in that oligomer. We determined all possible combinations of oligomer sizes for the 3- and 6-chain system. As an example we enumerated aggregation states for 3-chain system in Table I. Lower numbered aggregation states correspond to a less aggregated system, with 0 being the completely monomeric state. Conversely, the higher numbered aggregation states correspond to aggregated systems that include larger fragments. A similar casification was done for the 6-chain system while the aggregation behavior for the 12-chain system was characterized by tracking only the largest β-sheet in the system [22].

3. Results

We simulated 3-, 6-, and 12-chain GNNQQNY systems. We will first present the results of the 3- and 6-chain systems, as we have performed 3 and 12 runs for these systems, respectively, and can thus provide an in depth statistical analysis of the results. Conversely, because the computational cost of simulating the 12-chain system was high, we only performed one run for this system. WHAM [42] was used to calculate various quantities important for understanding the behavior of the system as a function of temperature T. In our study, we examined the temperature dependence of the heat capacity and the order parameters $\langle P_1 \rangle$ and $\langle P_2 \rangle$ as shown in Figure 1 for 3- and 6-chain systems. Fluctuations in energy (A and C) appear maximal at the transition point T_{trans}. The peaks in C_v for the 3-chain system in (A) occurs at $T_{\text{trans}} \approx 0.86$ RTU and for the 6-chain system in (C) at $T_{trans} \approx 0.89$ RTU. From (B) and (D) we notice that $\langle P_1 \rangle$ and $\langle P_2 \rangle$ decrease over the entire temperature range with the sharpest decrease at the transition point. This link between change in energy and change in system order suggests aggregation into ordered structures at T_{trans}.

In order to understand how aggregation proceeds we discuss characteristic features of representative structures in the different phases (i.e. at the lowest temperature T_{low}, T_{trans}, and at the highest temperature T_{high}). Figure 2 displays typical structures of

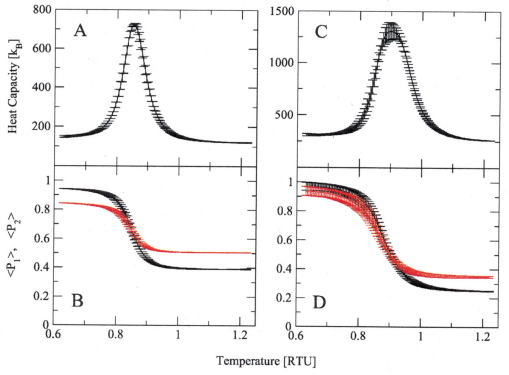

Figure 1: 3-chain system: C_v vs T (A) and $\langle P_{1,2}\rangle$ vs T (B). 6-chain system: C_v vs T (C) and $\langle P_{1,2}\rangle$ vs T (D). $\langle P_1\rangle$ is represented in black, while $\langle P_2\rangle$ is represented in red. Error bars represent standard deviations calculated from independent samples obtained in different runs.

the 3- and 6-chain systems for temperatures T_{low}, T_{trans}, and T_{high} together with the values for P_1 and P_2. The systems were all aggregated at T_{low}, partially associated at T_{trans}, and dissociated at T_{high}. At T_{low}, the systems are completely aggregated into mostly in-register, parallel, twisted β-sheets. Because these β-sheets are twisted, $\langle P_1\rangle \neq \langle P_2\rangle \neq 1$. At T_{trans}, the system is in transition between completely dissociated and completely associated, and between parallel order and disordered. At T_{high}, the systems are completely dissociated, and display very little ordering. The reason $\langle P_2\rangle$ is not zero at T_{high} is because of finite size effects, which have also been observed by Caflisch and coworkers in their study of GNNQQNY trimer formation using an atomic force field [13]. In the previous paragraph, it was noted that the peaks in C_v very nearly match the peaks in the fluctuation of $\langle P_1\rangle$ and $\langle P_2\rangle$. Here we see that the change in internal energy is caused by aggregation.

The aggregation pathway was analyzed to determine the mechanism of aggregation. The oligomers occurring during the aggregation of the 3- and 6-chain systems were assigned to physically intuitive aggregation states exemplified in Table I for the 3-chain system. Figure 3 shows the aggregation pathways as a function of temperature. For the 3-chain system, we see that at T_{low} the system is in a trimer conformation. Near T_{trans} the system visits all three aggregation states, each with similar probability. At T_{high} the system is in a 3-monomers conformation. Because we see a smooth change from three monomers to one trimer, we conclude that the GNNQQNY trimer prefers to associate via monomer addition rather than a condensation-ordering transition. This is because an initial condensation process would be practically replete of the intermediate (1 dimer and 1 monomer) configuration. Furthermore, we would expect to see two peaks in the C_v curve in Figure 1, one for condensation and another for reordering.

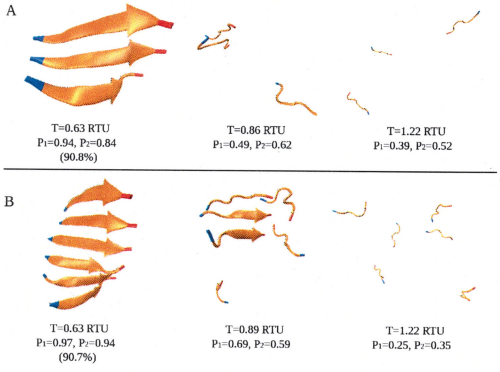

Figure 2: Representative structures at T_{low} (left), T_{trans} (mid), and T_{high} (right) are shown for (A) the 3-chain system, and (B) the 6-chain system. For the structures at T_{low} we included the Boltzmann populations (in parantheses) of the conformations at the given P_1 and P_2 values ± 0.05.

For the 6-chain system, we see that at T_{low} the system is in a hexameric conformation. Near T_{trans} the system occupies every state; only the configuration consisting of a monomer, a dimer and a trimer (aggregation state 4) is noticeably suppressed. At T_{high} the system is either in a 6-monomers configuration with the highest probability, or in a 4-monomers and 1-dimer configuration. As with the 3-chain system, the 6-chain system visits many intermediate states. This suggests that the system does not undergo an initial condensation, and instead aggregates via a different mechanism. One possibility is monomer addition, but there is also the possibility of two small oligomers aggregating into a larger oligomer, which we call oligomer fusion [43].

In addition to the 3- and 6-chain systems we performed a single 12-chain simulation for 500 ns per replica. For this system we observed the peak in the heat capacity at $T = T_{\text{trans}} = 0.95$ RTU (data not shown), which suggests that with increasing system

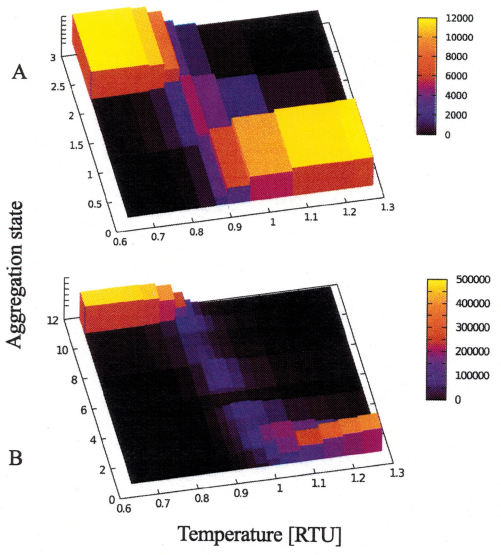

Figure 3: The aggregation pathway of GNNQQNY for the (A) 3- and (B) 6-chain systems. The depth axis is a measure of aggregation. Along the wide axis is T, and along the tall axis is the population of the given state. The sum of the population across all states at any given T is constant.

size aggregation occurs at higher temperatures. Although the 12-chain C_v is similar to 3- and 6-chains, the behavior of $P_{1,2}$ is dramatically different (Figure 4). At low temperatures we see a marked bimodal distribution of P_1 and P_2, indicating that the system has two different behavioral phases. This behaviour is explained by two different types of structures (Figure 5). The low P_2 value corresponds to two stacked β-sheets with an almost perpendicular relative orientation with respect to each other. The high P_2 value corresponds to twelve chains aligned in one parallel β-sheet. At T_{trans}, we see many small oligomers that have broken apart from the larger β-sheets aggregates, giving rise to the relatively flat P_1 and P_2 distributions. At T_{high}, we see that the 12-chain system is completely dissociated and disordered.

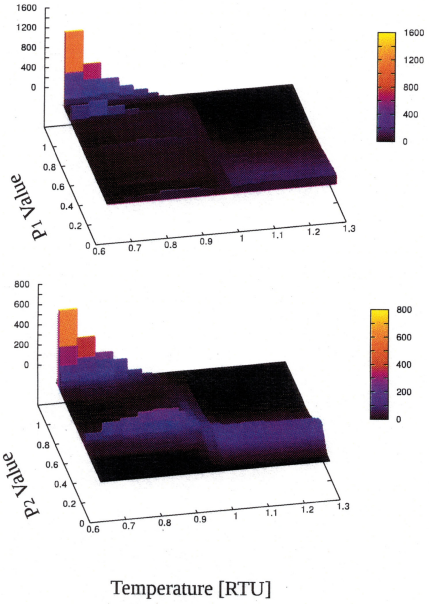

Figure 4: Histogram in dependence of P_1 and T (A) and P_2 and T (B) for the 12-chain GNNQQNY system.

The aggregation pathway of the 12-chain GNNQQNY system was defined by tracking only the largest β-sheet (Figure 5A). At T_{low} the largest β-sheet in the system is either a dodecameric, heptameric, or hexameric conformation. Near T_{trans}, all oligomers ranging from a dodecamer down to monomers are populated, but with the highest populations being observed for the hexamer

and heptamer. At T_{high} the largest β-sheet species is either a monomer, dimer, or trimer, with the probability of twelve monomers being the highest. Since all β-sheet sizes are observed over the temperature range, we conclude that large GNNQQNY aggregates also do not form by hydrophobic collapse. However, unlike the 3- and 6-chain systems, the 12-chain system does not ramp up smoothly from a dimeric to a dodecameric β-sheet. Furthermore, we conclude that the aggregation into a single sheet occurred via β-sheet fusion, where two smaller aggregates, e.g., two 6-chain sheets or a 7- and a 5-chain sheet coming together. β-sheet fusion is evidenced by the relative lack of abundance of 8–11 chain β-sheets, which would be expected to occur much more often if the aggregation from 7 chains to 12-chains was done via monomer addition.

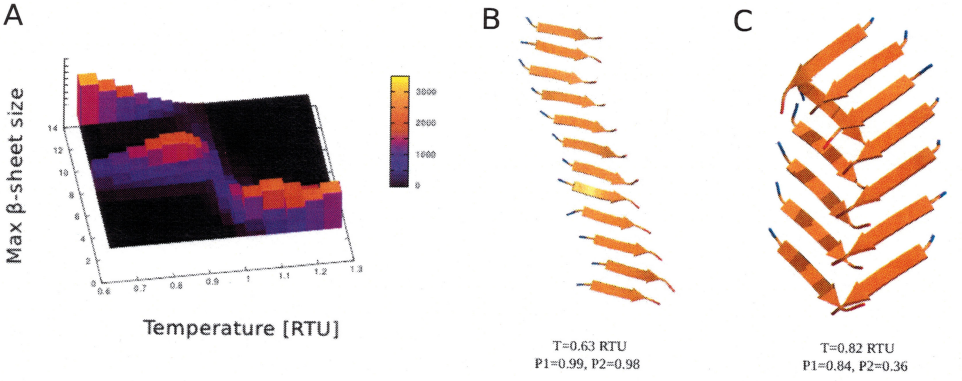

Figure 5: (A) Aggregation states of 12-chain GNNQQNY in terms of β-sheet size in dependence of temperature. (B) and (C) Typical structures of 12-chain GNNQQNY at $T < T_{\text{low}}$.

4. Discussion and conclusions

The self-assembly of peptides and proteins into soluble oligomers that evolve to protofibrils and eventually to fibrils is still challenging to study at atomic resolution using experimental approaches. Molecular simulations help reveal the molecular mechanism of the multi-step process of amyloid aggregation, elucidating structural and kinetic information about this process. The aim of the present work is to characterize structural transitions involved in oligomer formation for the model peptide GNNQQNY.

Our results clearly show that GNNQQNY has a strong propensity to form stable β-sheets independent of its oligomeric state. This observation is in agreement with the result of previous simulation studies investigating GNNQQNY oligomerization, ranging from dimer, trimer and tetramer formation using atomic force fields [12, 13, 15, 16, 18] to the aggregation into 12-mers and 20-mers employing a coarse-grained protein model [21]. Our REMD study leads to an almost exclusive population of parallel β-sheets independent of the oligomer size in agreement with experimental findings [8–11, 18] and simulation studies [18, 21]. The deficiency of antiparallel β-sheets can be attributed to the lack of charged termini in our study in contrast to CG studies by Mousseau and coworkers [21] and most of the atomic simulations [12, 13, 15–20] that used charged termini to study GNNQQNY aggregation.

The structural and aggregate-state analysis of our REMD data for 3-, 6-, and 12-chain GNNQQNY system revealed that changes in oligomer size and peptide order correspond to a single change in the heat capacity, C_v. GNNQQNY self-assembles into parallel β-sheets at the transition temperature T_{trans} of 225–285 K. The absence of further C_v peaks, along with the temperature dependence of the order parameters $\langle P_1 \rangle$ and $\langle P_2 \rangle$ further evidence that aggregation and β-sheet-formation occur at the same temperature, implying unordered GNNQQNY aggregates are thermodynamically unstable. The observation of only one heat capacity peak during the aggregation of GNNQQNY followed by REMD simulations is confirmed by other computational studies [13, 16, 21].

For the 3- and 6-chain systems, GNNQQNY aggregates into one long β-sheet as the system is cooled. In both cases, all oligomer sizes are visited during the formation of the trimeric and hexameric β-sheet, respectively. The comparison with the order parameters $\langle P_1 \rangle$ and $\langle P_2 \rangle$ and the single C_v peak already revealed that aggregation and β-sheet formation occur at the same temperature. We can therefore conclude that the oligomerization into small β-sheets proceeds via monomer addition to existing β-sheets and fusion of smaller β-sheets. For the 12-chain system, GNNQQNY aggregates either into a single 12-mer β-sheet or into a double-layered β-sheet with the two β-sheets being of similar size. For this system the probability for the β-sheets consisting of 8 to 11 peptides is considerably reduced compared to the smaller and dodecameric β-sheets. We can therefore conclude that first β-sheets with a high preference for 5-mers, 6-mers and 7-mers are formed, which then aggregate into a single- or double-layered 12-mer. The final stable structures, which we obtain for the 12-mer, are very similar to those found with OPEP, apart from the orientation of the strands within the sheets [21].

The main conclusion from our study is that the aggregation of the hydrophilic GNNQQNY sequence is mainly driven by H-bond formation, leading to the formation of β-sheets from the very beginning of the assembly process. The preceding condensation step, resulting in amorphous aggregates as observed for amyloidogenic hydrophobic peptides, does not occur for

GNNQQNY. Instead, condensation (aggregation) and ordering take place simultaneously. This is evidenced by a single peak in the heat capacity curve for GNNQQNY assembly [16, 21].

Acknowledgments

MB acknowledges support by NSF Grant DMR-1207437.

[1] Selkoe DJ. Folding proteins in fatal ways. Nature 2003;426:900–904.
[2] Chiti F, Dobson CM. Protein misfolding, functional amyloid, and human disease. Annu Rev Biochem 2006;75:333–366.
[3] Uversky VN, Fink AL. Protein misfolding, aggregation and conformational disease. Springer. 2006.
[4] Walsh DM, Klyubin I, Fadeeva JV, Cullen WK, Anwyl R, Wolfe MS, Rowan MJ, Selkoe DJ. Naturally secreted oligomers of amyloid β protein potently inhibit hippocampal long-term potentiation *in vivo*. Nature 2002;416:535–539.
[5] Kirkitadze MD, Bitan G, Teplow DB. Paradigm shifts in Alzheimers disease and other neurodegenerative disorders: the emerging role of oligomeric assemblies. J Neurosci Res 2002;69:567–577.
[6] Bucciantini M, Giannoni E, Chiti F, Baroni F, Formigli L, Zurdo J, Taddei N, Ramponi G, Dobson CM, Stefani M. Inherent toxicity of aggregates implies a common mechanism for protein misfolding diseases. Nature 2002;416:507–511.
[7] Klein WL, Stine WB, Teplow DB. Small assemblies of unmodied amyloid β-protein are the proximate neurotoxin in Alzheimers disease. Neurobiol Aging 2004;25:569–580.
[8] Balbirnie M, Grothe R, Eisenberg DS. An amyloid-forming peptide from the yeast prion Sup35 reveals a dehydrated β-sheet structure for amyloid. Proc Natl Acad Sci USA 2001;98:2375–2380.
[9] Nelson R, Sawaya MR, Balbirnie M, Madsen AØ, Riekel C, Grothe R, Eisenberg D. Structure of the cross-β spine of amyloid-like fibrils. Nature 2005; 435:773–778.
[10] Sawaya MR, Sambashivan S, Nelson R., Ivanova MI., Sievers SA, Apostol MI, Thompson MJ, Balbirnie M, Wiltzius JJ, McFarlane HT, Madsen AØ, Riekel C., Eisenberg D. Atomic structures of amyloid cross-beta; spines reveal varied steric zippers. Nature 2007;447:453–457.
[11] van der Wel PCA, Lewandowski JR, Griffin RG. Structural characterization of GNNQQNY amyloid fibrils by magic angle spinning NMR. Biochemistry 2010;49:9457–9469.
[12] Gsponer J, Haberthür U, Caflisch A. The role of side-chain interactions in the early steps of aggregation: Molecular dynamics simulations of an amyloid-forming peptide from the yeast prion Sup35. Proc Natl Acad Sci USA 2003;100:5154–5159.
[13] Cecchini M, Rao F, Seeber M, Caflisch A. Replica exchange molecular dynamics simulations of amyloid peptide aggregation. J Chem Phys 2004; 121:10748.
[14] Zheng J, Ma B, Tsai CJ, Nussinov R. Structural stability and dynamics of an amyloid-forming peptide GNNQQNY from the yeast prion Sup-35. Biophysics Journal 2006;91:824–833.
[15] Zhang Z, Chen H, Bai H, Lai L. Molecular dynamics simulations on the oligomer-formation process of the GNNQQNY peptide from yeast prion protein Sup35. Biophys J 2007;93:1484–1492.
[16] Strodel B, Whittleston CS, Wales DJ. Thermodynamics and kinetics of aggregation for the GNNQQNY peptide. J Am Chem Soc 2007;129:16005–16014.
[17] Meli M, Morra G, Colombo G. Investigating the mechanism of peptide aggregation: Insights from mixed Monte Carlo-molecular dynamics simulations. Biophysical J 2008;94:4414–4426.
[18] Vitagliano L, Esposito L, Pedone C, de Simone A. Stability of single sheet GNNQQNY aggregates analyzed by replica exchange molecular dynamics: Antiparallel versus parallel association. Biochem Biophys Res Commun 2008;377:1036 – 1041.
[19] Park J, Kahng B, Hwang W. Thermodynamic selection of steric zipper patterns in the amyloid cross-β spine. PLoS Comput Biol 2009;5:e1000492.
[20] Reddy AS, Chopra M, de Pablo J.J. GNNQQNY-investigation of early steps during amyloid formation. Biophysical J 2010;98:1038–1045.
[21] Nasica-Labouze J, Meli M, Derreumaux P, Colombo G, Mousseau N. A multiscale approach to characterize the early aggregation steps of the amyloid-forming peptide GNNQQNY from the yeast prion sup-35. PLoS Comput Biol 2011;7:e1002051.
[22] Osborne KL, Bachmann M, Strodel B. Thermodynamic analysis of structural transitions during GNNQQNY aggregation. Proteins: Struct, Func and Bioinf 2013;DOI: 10.1002/prot.24263.
[23] Sugita Y, Okamoto Y. Replica-exchange molecular dynamics method for protein folding. Chem Phys Lett 1999;314:141–151.
[24] Pellarin R, Caflisch A. Interpreting the aggregation kinetics of amyloid peptides. J Mol Biol 2006;360:882–892.
[25] Pellarin R, Guarnera E, Caflisch A. Pathways and intermediates of amyloid fibril formation. J Mol Biol 2007;374:917–924.
[26] Magno A, Caflisch A, Pellarin R. Crowding effects on amyloid aggregation kinetics. J Phys Chem Lett 2010;1:3027–3032.
[27] Bellesia G, Shea JE. Self-assembly of β-sheet forming peptides into chiral fibrillar clusters. J Chem Phys 2007;126:245104.
[28] Bellesia G, Shea JE. Effect of β-sheet propensity on peptide aggregation. J Chem Phys 2009;130:145103.
[29] Nguyen HD, Hall CK. Molecular dynamics simulations of spontaneous fibril formation by random-coil peptides. Proc Natl Acad Sci USA 2004;101:16180–16185.
[30] Nguyen HD, Hall CK. Spontaneous fibril formation by polyalanines; discontinuous molecular dynamics simulations. J Am Chem Soc 2006;128:1890–1901.
[31] Cheon M, Chang I, Hall CK. Extending the PRIME model for protein aggregation to all 20 amino acids. Proteins: Struct, Func and Bioinf 2010;78:2950–2960.
[32] Urbanc B, Cruz L, Ding F, Sammond D, Khare S, Buldyrev SV, Stanley HE, Dokholyan NV. Molecular dynamics simulation of amyloid β dimer formation. Biophys J 2004;87:2310–2321.
[33] Urbanc B, Betnel M, Cruz L, Bitan G, Teplow DB. Elucidation of amyloid β-protein oligomerization mechanisms: Discrete molecular dynamics study. J Am Chem Soc 2010;132:4266–4280.
[34] Derreumaux P. From polypeptide sequences to structures using Monte-Carlo simulations and an optimized potential. J Chem Phys 1999;111:2301–2310.
[35] Melquiond A, Boucher G, Mousseau N, Derreumaux P. Following the aggregation of amyloid-forming peptides by computer simulations. J Chem Phys 2005;122:174904.
[36] Derreumaux P, Mousseau N. Coarse-grained protein molecular dynamics simulations. J Chem Phys 2007;126:025101.
[37] Maupetit J, Tuffery P, Derreumaux P. A coarse-grained protein force field for folding and structure prediction. Proteins: Struct, Func and Bioinf 2007; 69:394–408.
[38] Bereau T, Deserno M. Generic coarse-grained model for protein folding and aggregation. J Chem Phys 2009;130:235106.
[39] Bereau T, Bachmann M, Deserno M. Interplay between secondary and tertiary structure formation in protein folding cooperativity. J Am Chem Soc 2010; 132:13129–13131.
[40] Bereau T, Globisch C, Deserno M, Peter C. Coarse-grained and atomistic simulations of the salt-stable Cowpea chlorotic mottle virus (ss-ccmv) subunit 2649: β-barrel stability of the hexamer and pentamer geometries. J Chem Theory Comput 2012;8:3750–3758.
[41] Limbach HJ, Arnold A, Mann BA, Holm C. ESPResSo - an extensible simulation package for research on soft matter systems. Comp Phys Comm 2006; 174:704–727.
[42] Kumar S, Bouzida D, Swendsen RH, Kollman PA, Rosenberg JM. The weighted histogram analysis method for free-energy calculations on biomolecules. 1: The method. J Comp Chem 1992;13:1011–1021.
[43] Hill SE, Robinson J, Matthews G, Muschol M. Amyloid Protofibrils of Lysozyme Nucleate and Grow Via Oligomer Fusion. Biophys J 2009;96:3781–3790.